Research paper

Perforation analysis of S235 steel sheets up to 573 K using experimental and numerical methods

M. Klosak[1], M. Grazka[2], L. Kruszka[3], W. Mocko[4]

Abstract: This paper reports on efficient experimental and numerical techniques used in the design of critical infrastructure requiring special protection measures regarding security and safety. The presented results, some of which have already been reported in [1], were obtained from perforation experiments carried out on S235 steel sheets subjected to impacts characterized as moderate velocity (approximately 40–120 m/s). The metal was tested using the Hopkinson Bar Technique and pneumatic gun. The originality of perforation testing consist on using a thermal chamber designed to carry out experiments at higher temperatures. 3D scanners and numerically controlled measuring devices were used for the final shape deformation measurements. Finally, the results of FEM analysis obtained using explicit solver are presented. The full-scale CAD model was used in numeric calculations.

Keywords: steel perforation, ballistic properties, FEM analysis, CNC measuring

[1] PhD., Eng., Universiapolis, Technical University of Agadir, Technopole d'Agadir, Qr Tilila, 80000 Agadir, Morocco, e-mail: klosak@e-polytechnique.ma, ORCID: https://orcid.org/0000-0001-6763-9704

[2] PhD., Eng., Military University of Technology, Faculty of Mechatronics, Armaments and Aviation, ul. gen. Sylwestra Kaliskiego 2, 00-908 Warsaw, Poland, e-mail: michal.grazka@wat.edu.pl, ORCID: https://orcid.org/0000-0003-0639-5755

[3] PhD., Eng., Military University of Technology, Faculty of Civil Engineering and Geodesy, ul. gen. Sylwestra Kaliskiego 2, 00-908 Warsaw, Poland, e-mail: leopold.kruszka@wat.edu.pl, ORCID: https://orcid.org/0000-0001-5129-2531

[4] DSc., PhD., Eng., Motor Transport Institute, Center for Material Testing, Jagiellońska 80, 03-301 Warsaw, Poland, e-mail: wojciech.mocko@its.waw.pl, ORCID: https://orcid.org/0000-0002-6845-5453

1. Introduction

The material under investigation, i.e. S235 steel, is a typical construction material. The S235 steel tested under perforation investigation, subjected to impacts of moderate velocity [2] is a typical building material. Much has been said about its application in construction where this kind of steel is widely used for the manufacture of frames or façade panels, including steel protective doors [3]. However, its mechanical properties are also beneficial for the development of engineering applications in the domain of the so-called critical infrastructure.

The security of critical infrastructure has become more of a concern at a time of increasing terrorist threats. The term itself refers to the following facilities and their components: structures related to production, transmission, and distribution of electricity, fuels, crude oil and petroleum products, telecommunication infrastructure, water installations, food production, and distribution centers, heating facilities, health care facilities (hospitals), transport (roads, railway, airports, ports), financial institutions and security services (police, army, rescue services) [4–6]. Thus, the critical infrastructure includes not only military buildings, but also public utility buildings which are made of typical building materials such as used S235 steel. These facilities are crucial to be secured for the proper functioning of the country. It is, therefore, necessary to implement sophisticated and efficient policies and systems to protect this infrastructure. It is obvious this protection shall be provided with reliable engineering structures for which protective capabilities of construction materials have been fully assessed.

It is to be noted that a danger to critical infrastructure elements does not usually come from a direct missile attack, but it is mainly caused by debris from an explosion or ricochet. As the whole building cannot be protected against a missile attack, engineers design special reinforcements consisting of metal plates or composite elements for doors, walls etc. This is where the S235 steel sheets have their applicability.

2. Laboratory set-up and experimental data

2.1. Material and specimen description

Laboratory tests of S235 (also designated as A283C in ASME standards) steel sheets and numerical calculations of dynamic perforation of the specially prepared specimens were conducted using measuring devices available in three different research centers. Sheet metal perforation tests were

performed in the dynamic research laboratory at the Universiapolis of Agadir (Morocco). Tensile tests on this steel were carried out at the Motor Transport Institute (Warsaw, Poland) and the measurements of the deformed samples as well as numerical simulations using the FEM method were made at the Institute of Armament at the Military University of Technology (Warsaw, Poland).

The chemical composition of structural steel is extremely important and regulated by codes. It is a fundamental factor which defines the mechanical properties of the steel material. Table 1 presents maxima percentage levels of certain regulated elements as chemical components required for S235 according to the European standards.

Table 1. Chemical composition of structural steel S235 [7]

Chemical composites	C %	Mn %	P %	S %	Si %
Steel S235	0,22	1,60	0,05	0,05	0,05

The mechanical properties of structural steel are fundamental to its classification and hence application. Even though the chemical composition is a dominant factor of the mechanical properties of steel, it is also very important to understand the minimum standards for the mechanical properties. The naming convention used in European Standard EN10025 refers to the minimum yield strength of the steel grade tested at 16 mm thick specimens. Table 2 presents the mechanical properties of the analyzed material.

Table 1. Steel S235 yield and tensile strength [7]

Structural steel	Minimum yield strength at nominal thickness 16 mm	Tensile strength at nominal thickness between 3 and 16 mm
	MPa	MPa
S235	235	360-510

The use of plate specimens subjected to perforation in gas guns [8, 9] or Hopkinson bars [10] are the most common experimental techniques to study ballistic properties of materials and structures. Usually, it is not possible to run an extended study on real-size specimens for economic and logistic reasons, therefore reference testing tools are used in experiments. The studied specimens are fully clamped in a rigid and solid frame with no free degrees of freedom. The aim of the study is to analyze different failure modes in which petaling is a common occurrence. The experiment is subjected to the numerical validation which allow to define a material model and, as a consequence, run full-scale models and verify real structure conditions.

The square steel sheet specimens 130 × 130 mm with two different thicknesses of 0.6 mm and 1.0 mm were used during the laboratory tests using the pneumatic gun. The cylindrical steel projectiles with a diameter of 11.5 mm and a conical tip ($\varphi = 72°$) with the weight of 28 g were used. These tests were carried out for two initial temperatures: room temperature $T_0 = 293$ K (20°C) and a higher temperature of $T_0 = 573$ K (300°C). The plates were mounted respecting the conditions of full fixation at all four sides as schematically shown in Fig. 1, together with the specimen and projectile geometry.
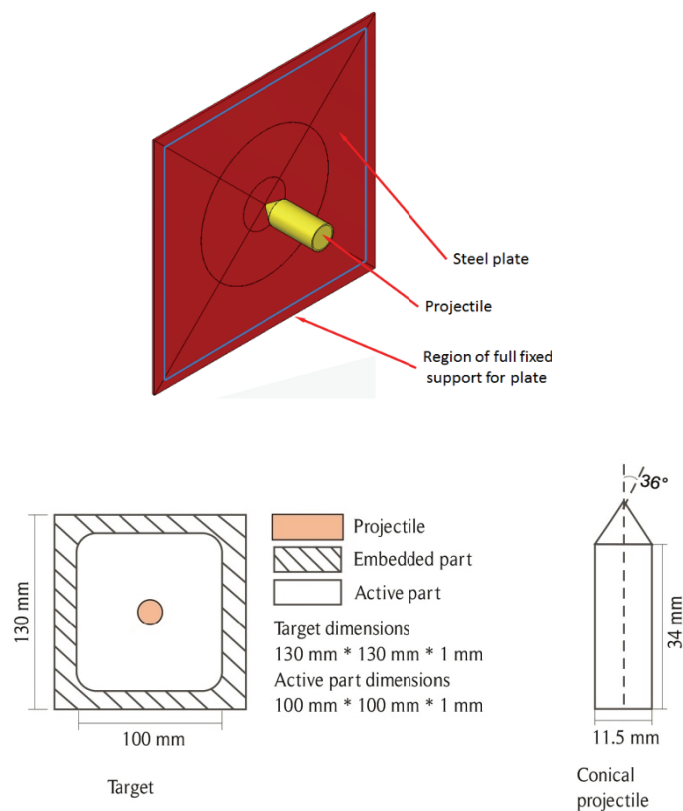

Fig. 1. Plate-projectile configuration during the laboratory experiments

2.2. Experimental set-ups

Three experimental set-ups were used in the experimental study. Figure 2 demonstrates the SHPB (Split Hopkinson Pressure Bar) system used in the dynamic material analysis for S235 steel [11–14]. The CNC measuring machine used for plate specimen's deformation analysis is presented in Fig. 3. The key dynamic study was carried out using a pneumatic gun which photo and scheme are presented in Fig. 4. A wide range of impact velocities from 40 m/s to 120 m/s has been covered during the perforation tests.

Fig. 2. Hopkinson Pressure Bar set-up for investigation of the material's dynamic behavior [11]

Fig. 3. CNC measuring machine used for plate deformation calculations [11]
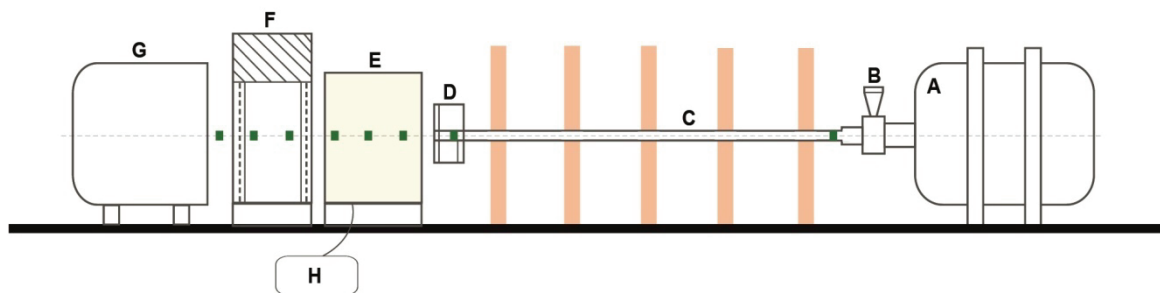
a)

A – pneumatic chamber, B – fast valve, C – gas gun tube with supports, D – sensor for initial impact velocity measurements, E – thermal chamber and specimen fixation device, F – sensor for residual velocity measurement, G – projectile catcher, H – PID controller, ■ ■ ■ projectile trajectory

b)

Fig. 4. Gas gun set-up used for perforation tests at high impact velocities and temperatures [8]; a) general

scheme, b) photo of the system with the installed thermal chamber

The apparatus is equipped with a thermal chamber in which a specimen is heated. Few experimental data are available in the international literature which deals with impact loading at elevated temperatures. This is due mainly to the non-coupling of standard gas gun with a heating tool. The usual approach is to carry out perforation tests at room temperature and to extrapolate results using numerical simulations at high temperatures by applying the defined constitutive relation. The temperature is modulated from room temperature to the maximum temperature of $T_0 = 573$ K (300°C). The air flows inside the system through to a ventilator. A sarcophagus is used around the plate specimen to keep a uniform temperature distribution. Therefore, the two sides of the specimen are heated up at the same time. Due to conductivity, the entire specimen reaches the initial temperature imposed to the specimen and regulated by a controller. A detailed description of the thermal chamber is given in [8], whereas Figure 5 presents the general principle of its functioning. The thermal chamber has been patented in Morocco under the reference number MA 41357 A1 (OMPIC), the extended experimental analysis using this set-up can be found in [15, 16].
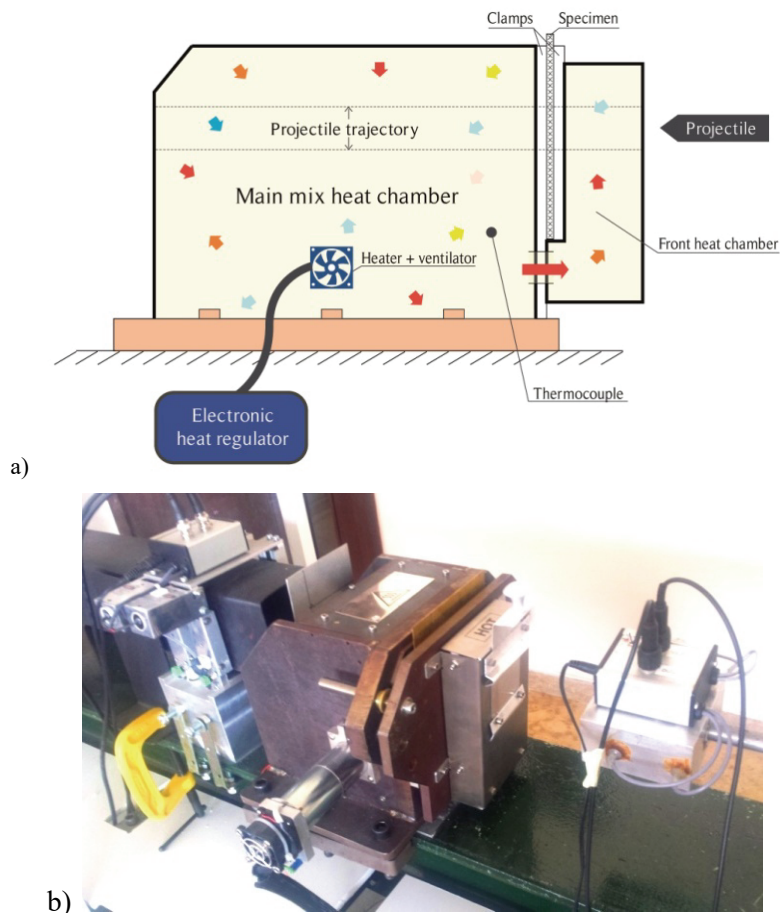

Fig. 5. Thermal chamber for heating up the target plate specimens; a) schematic representation of the air mixing process [8], b) general view of the thermal chamber

3. Results of laboratory experiments

3.1. Dynamic analysis of S235 steel properties

Many authors dealt with perforation analysis of steel plates, from theoretical approaches such as discussed in [17] to more practical considerations as reported in [9, 18] where experimental results and numerical applications are discussed.

The perforation laboratory tests were carried out for two types of steel sheet thicknesses with a projectile initial impact velocity V_0 ranging from 40 to 120 m/s at two different thermal conditions $T_0 = 293$ K and $T_0 = 573$ K. During the tests, the initial velocity (V_0) of the projectile was measured at the moment of impact and the residual velocity (V_R) just after the specimen was perforated. Two separate laser sensor systems were used for the velocity quotes. The results of these measurements are recapitulated in Table 3.

Table 3. Impact velocity (V_0) and residual velocity (V_R) measured for ballistic perforation test

Specimen thickness 0.6 mm						Specimen thickness 1.0 mm					
Test no	Pressure [bar]	Temp. [K]	Impact velocity V_0 [m/s]	Time [ms]	Residual velocity V_R [m/s]	Test no	Pressure [bar]	Temp. [K]	Impact velocity V_0 [m/s]	Time [ms]	Residual velocity V_R [m/s]
T10	1.0	293	44.17	2.480	20.16	T2	2.0	293	64.93	–	0.00
T9	1.5	293	54.11	1.440	34.72	T3	3.0*	293	79.11	0.000	0.00
T8	2.0	293	64.43	1.080	46.30	T6	3.2	293	83.06	2.400	20.83
T7	3.0	293	79.11	0.740	67.57	T1	4.0	293	90.25	1.000	50.00
T12	4.0	293	90.58	0.640	78.13	T4	5.0	293	101.21	0.780	64.10
T13	5.0	293	100.40	0.540	92.59	T5	7.5	293	121.36	0.540	92.59
T14	7.5	293	121.36	0.440	113.64	T24	2.7**	573	75.50	0.000	0.00
T23	0.8	573	39.49	4.960	10.08	T25	3.0	573	79.11	1.440	34.72
T22	1.0	573	43.55	2.100	23.81	T26	4.0	573	91.24	0.830	60.24
T21	1.5	573	55.93	1.190	42.02	T27	5.0	573	101.62	0.660	75.76
T20	2.0	573	64.60	0.890	56.18	T28	7.5	573	122.55	0.490	102.04
T16	3.0	573	79.37	0.660	75.76	* perforated but with $V_R = 0$					
T17	4.0	573	90.91	0.570	87.72	** perforation but projectile stuck in specimen					
T18	5.0	573	100.81	0.490	102.04						
T19	7.5	573	120.77	0.430	116.28						

Figures 6 and 7 present the deformed specimens with a typical form of plate petaling. This behaviour is well known for steel and was reported in many works, the examples can be found in [19, 20].
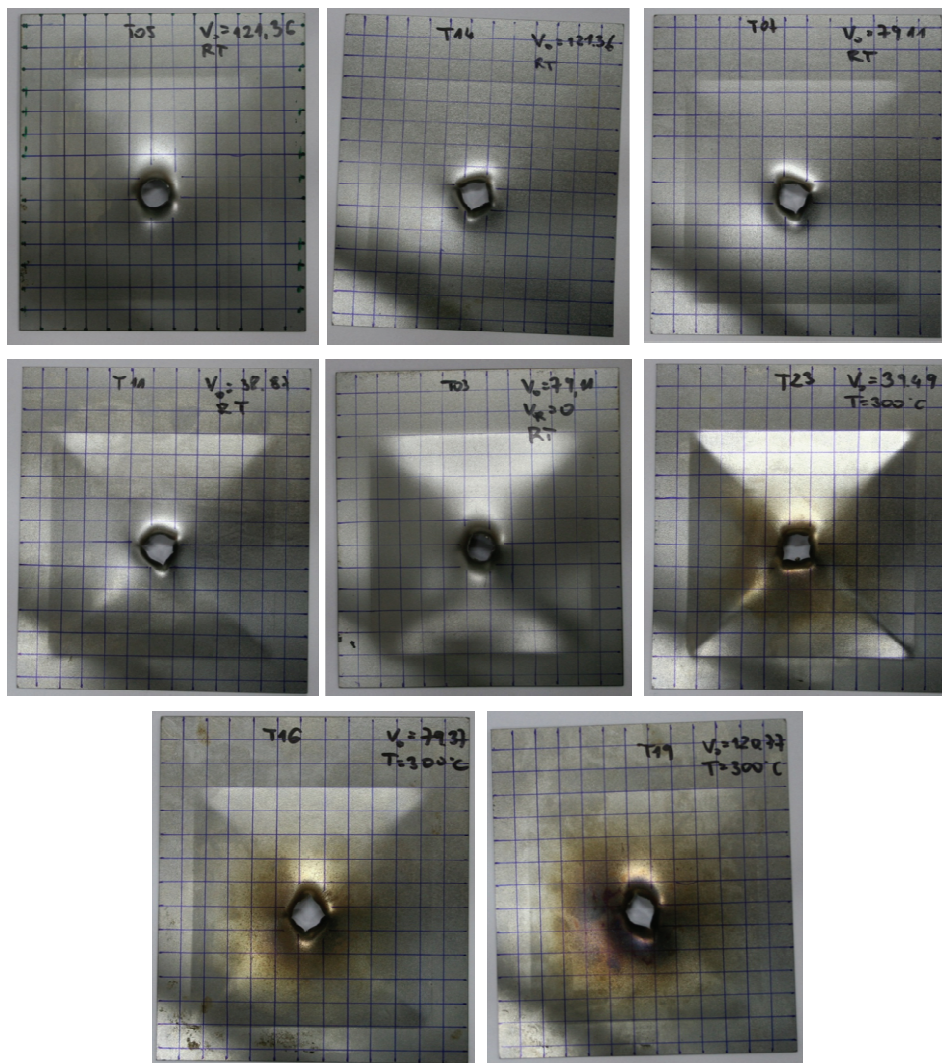

Fig. 6. Petaling as typical failure mode of perforation for tested metallic specimens at various initial impact velocity V_0; visible speckled traces of intensive heating in the thermal chamber at 573 K (300°C) as well as around shot holes including at room temperature RT as results of heating coming from both frictions during perforation phenomena by a projectile and from the dissipated plastic energy in the specimen material, i.e. so-called adiabatic heat effects

The final shape of the perforation holes presents 4 petals in almost all cases (Fig. 7). The tested specimens were submitted to further analysis in which the deformation shape was measured using

the CNC machines. Cross-sections of the target plates of thickness 1.0 mm after perforation are further illustrated in the macrographs as shown in Fig. 8 [21].
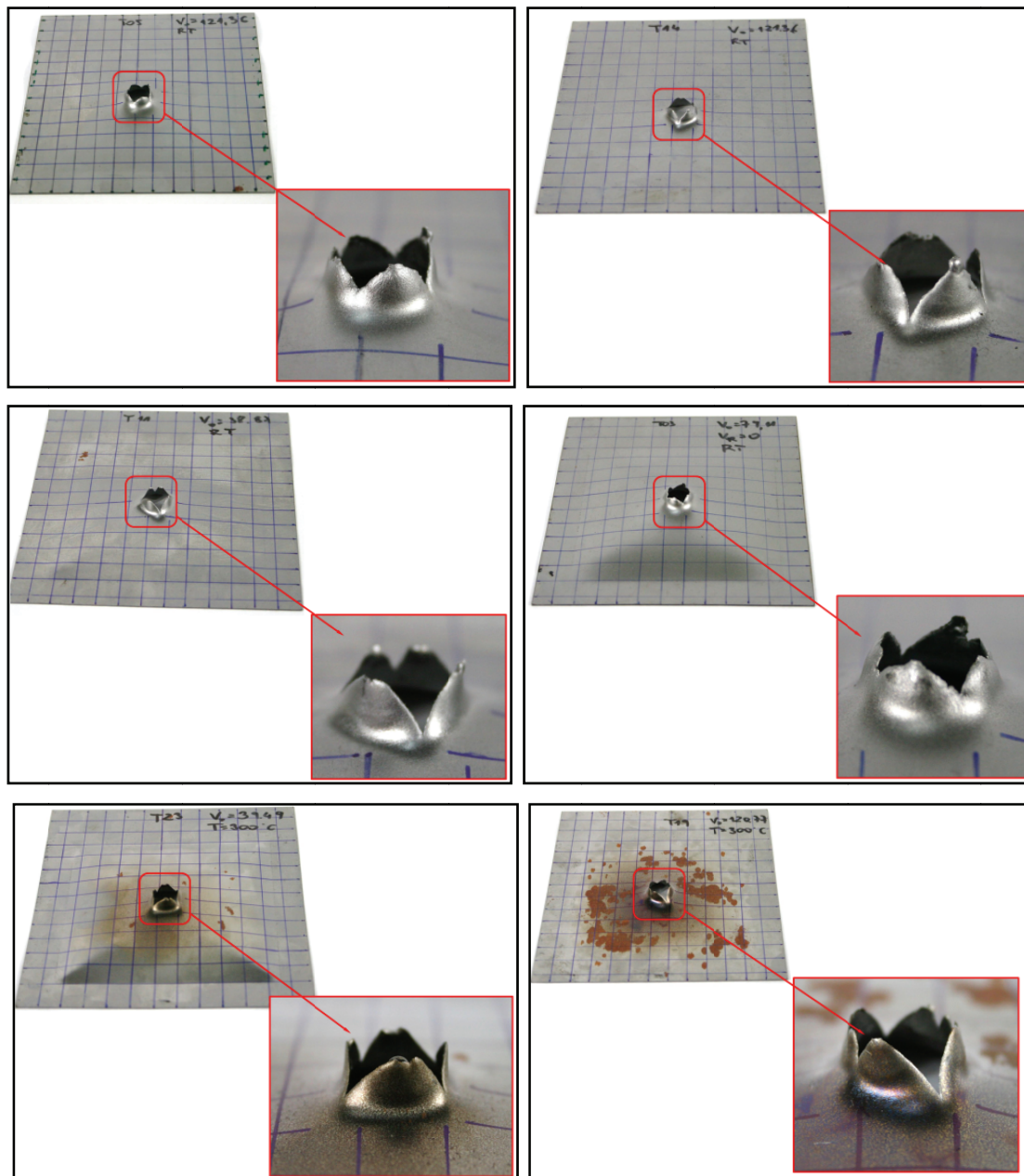

Fig. 7. Close-ups of different forms of petaling

It is to be noted that the plate thickness as well as the impact velocity had an influence on the final shape of the perforated specimen. The typical expected shapes are one-side convex (positive deformation – see Figs 8a and 8b. However, in case of $T_0 = 573$ K the final shape is different. The specimen received both positive and negative deformation (Figs 8c and 8d). It is anticipated this

was due to internal stresses caused by temperature. The maximum deformation measured is 4 mm. The measurements were identified later in numerical simulations.

Test Data:
Impact speed: ~79m/s
Residual speed: 0m/s
Temperature: 293K (20⁰C)
Plate thicknes: 1mm

Test Data:
Impact speed: ~121m/s
Residual speed: ~92m/s
Temperature: 293K (20⁰C)
Plate thicknes:1mm

Test Data:
Impact speed: ~38m/s
Residual speed: ~9m/s
Temperature: 293K (20⁰C)
Plate thicknes:0.6mm

Test Data:
Impact speed: ~121m/s
Residual speed: ~113m/s
Temperature: 293K
(20⁰C)
Plate thicknes:0.6mm

Test Data:
Impact speed: ~79m/s
Residual speed: ~75m/s
Temperature: 573K (300⁰C)
Plate thicknes:0.6mm

Test Data:
Impact speed: ~120m/s
Residual speed: ~116m/s
Temperature: 573K (300⁰C)
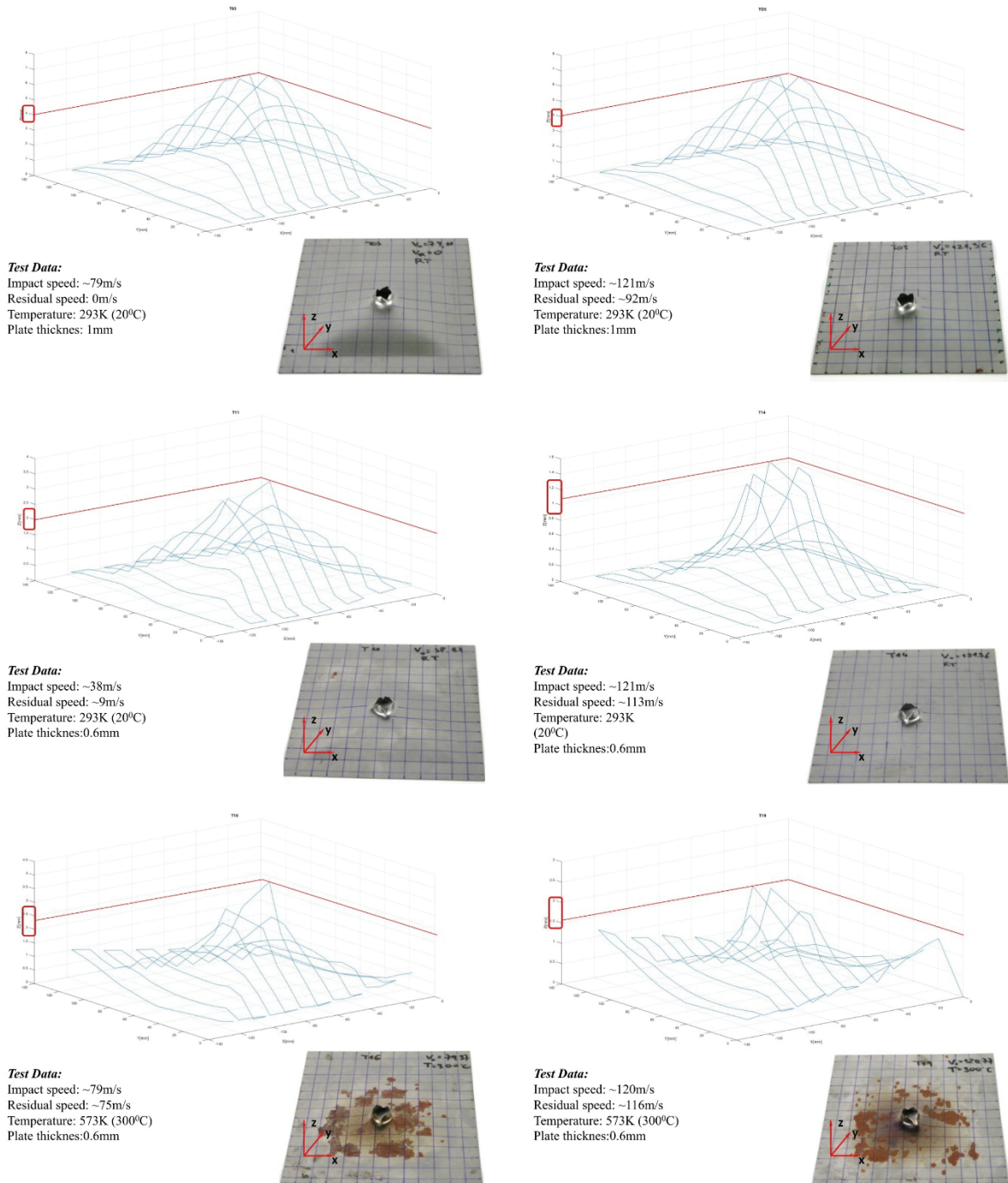Plate thicknes:0.6mm

Fig. 8. Deformed shape of plate specimens with measurements provided by CNC tool

Figure 9 reports a comparison between experimental results at $T_0 = 293$ K and $T_0 = 573$ K, all these experimental values were previously reported in Table 3. It can be noticed that increasing the initial temperature of the specimen shifts the ballistic limit (state of no perforation) to lower values. The

ballistic limits V_B obtained were approximately 42 m/s for $T_0 = 293$ K and subsequently they dropped to 37 m/s for $T_0 = 573$ K, this concerned the case of 0.6 mm plate. They were 82 m/s and 77 m/s, respectively, for 1.0 mm plate. The Recht-Ipson estimation [22] would suggest a slightly lower ballistic limit at for $T_0 = 293$ K, namely 75 m/s (compared to 77 m/s in the experiment). The other measured points are also shifted when higher residual velocities V_R are reported for elevated temperatures (see Fig. 9).
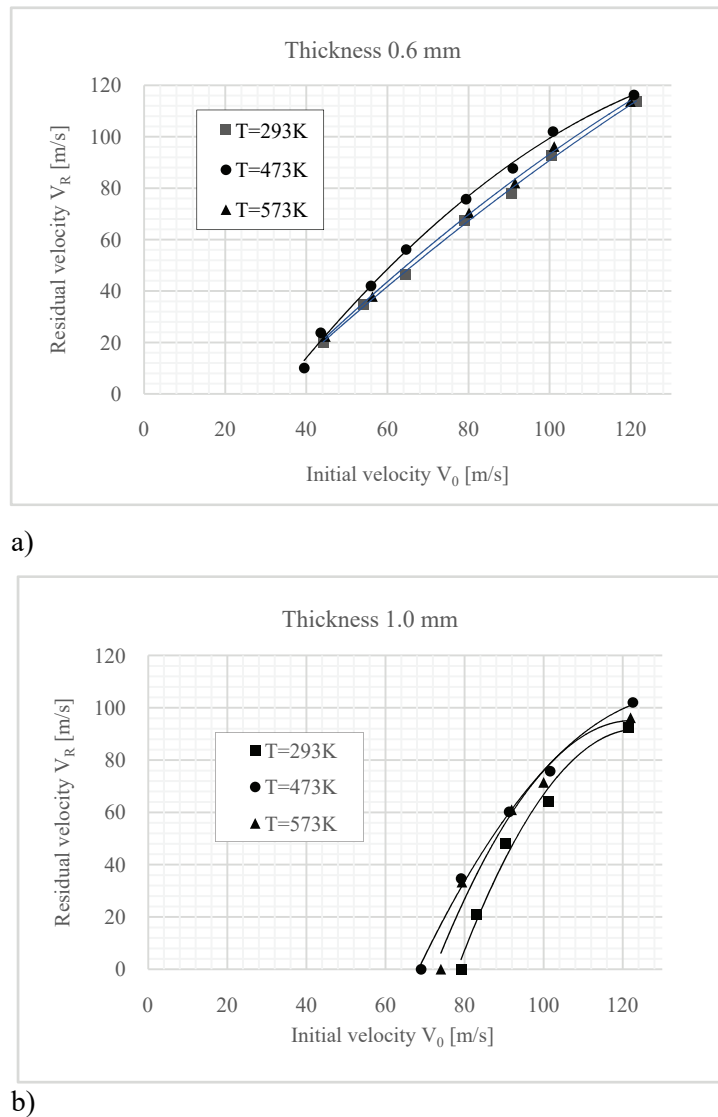

a)

b)

Fig. 9. Initial impact velocity V_0 vs. residual velocity V_R – experimental results for $T_0 = 293$ K and $T_0 = 593$ K; a) plate thickness of 0.6 mm, b) plate thickness of 1.0 mm

3.2. Kinetic energy calculation

The initial V_0 and residual V_R velocities were recorded during the tests, this information is useful for the kinetic energy estimation. The kinetic energy value demonstrates energy dissipation

capabilities of the material in dynamic loading. Figure 10 presents the percentage change in kinetic energy of the projectile for different impact velocities and for two temperatures of $T_0 = 293$ K and $T_0 = 573$ K. According to these records, the higher temperature decreases the protective capacity of S235 steel sheet. For the temperature difference of approximately $\Delta T = 280$ K this protective capacity is lowered by 5%. Also, the thickness of the steel sheet is important on the protective capacity. A greater thickness guaranties better protection ability. As observed in Fig. 10 the total differences in kinetic energy recorded for 0.6 mm and 1.0 mm steel sheets are 14% in favor of the thicker specimen.
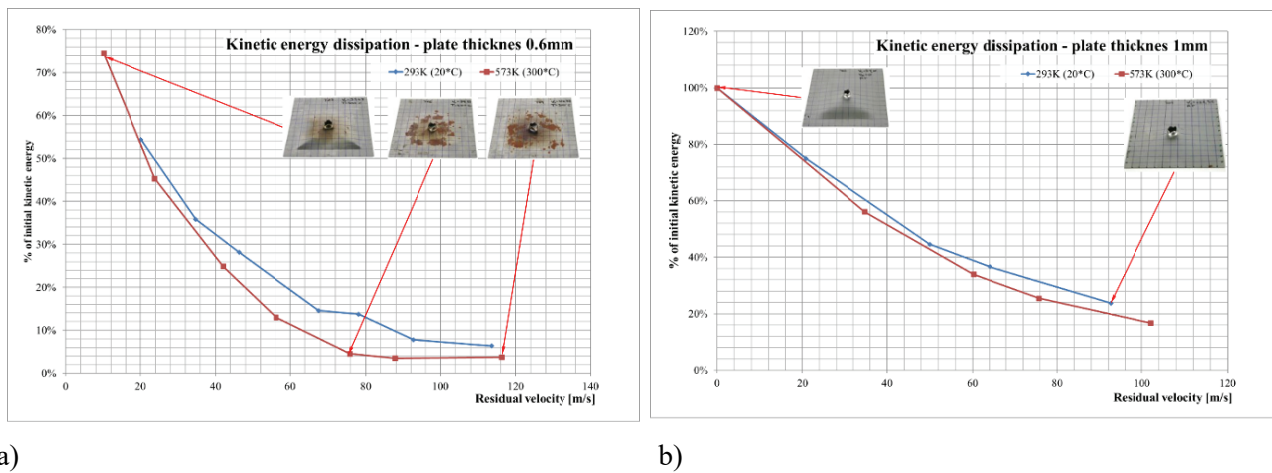

a)   b)

Fig. 10. Kinetic energy dissipation: $T_0 = 293$ K (20°C) vs. $T_0 = 573$ K (300°C); a) specimen thickness 0.6 mm, b) specimen thickness 1.0 mm

3.3. Analysis of the material anisotropy

Anisotropic properties of the steel sheet coming from rolling process may significantly affect material behaviour exposed to high velocity perforation. Various stress-strain characteristics and fracture strain depending on loading direction may result in both petaling formation and deflection of the sheet. Therefore, it is required to experimentally determine material anisotropy in order to avoid errors in numerical simulations.

The steel supplied for testing was delivered in the form of metal sheets. The sheets were subjected to a rolling process which could cause an anisotropy of properties. In order to investigate whether the phenomenon of anisotropy did not occur in the tested material, samples were cut at different angles regarding the rolling direction.

The tests were carried out using the samples cut in four directions: 0°, 30°, 60°, 90° in regard to the rolling direction. The tests were performed for different rates of deformation: 10^{-3} s^{-1}, 10^{-1} s^{-1}, 1 s^{-1}, 10 s^{-1}. The results shown in Fig. 11 confirm the analysis did not reveal any anisotropy.
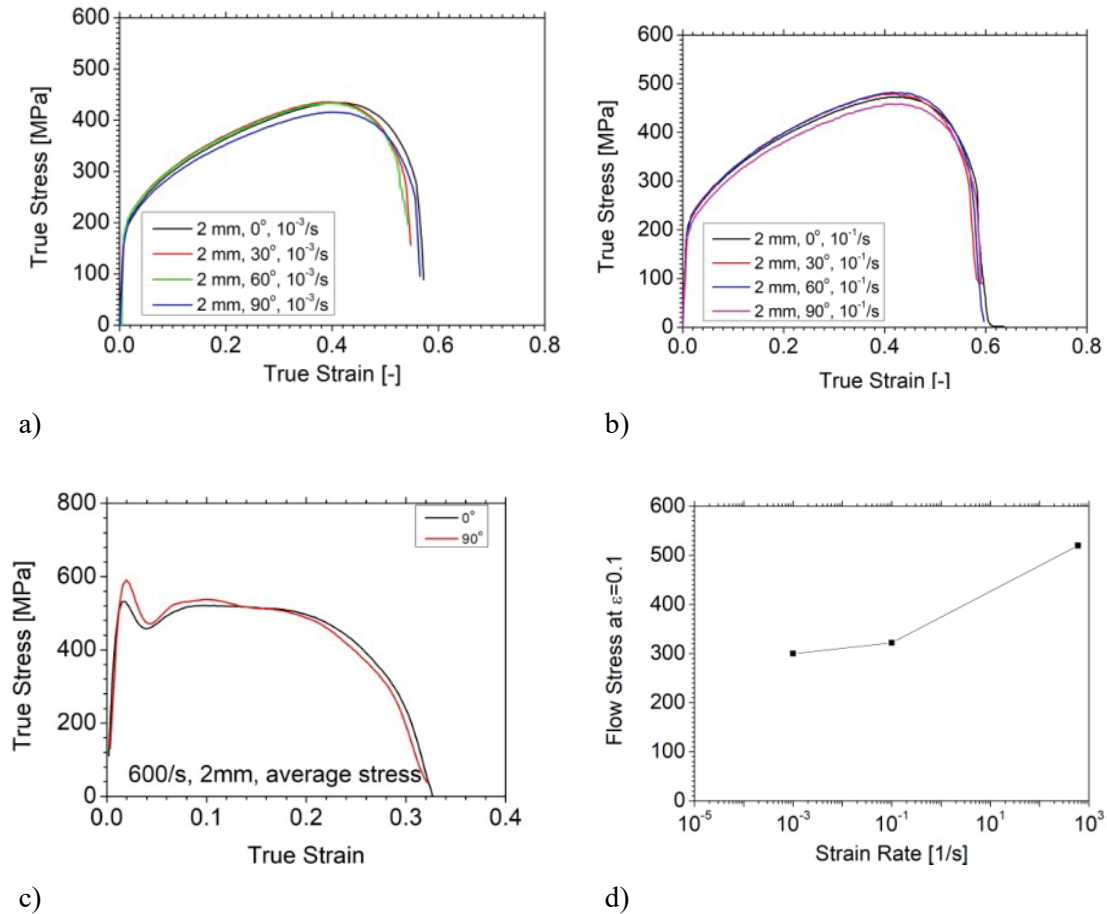

Fig. 11. Experimental results of tensile tests at various strain rates and different direction cut of the 2 mm material samples; a) static tests, b) quasi-static tests, c) dynamic tests, d) flow stress at 10% true strain vs strain rate for 0° direction

4. Numerical simulations using FEM method

4.1. Initial and boundary conditions

Numerical calculations were performed using Ansys explicit solver dedicated for high rates of deformations in line with the practice used in many previous works [18, 23, 24]. In all calculations, the S235 steel sheet and projectile were modelled as presented in Fig. 12.
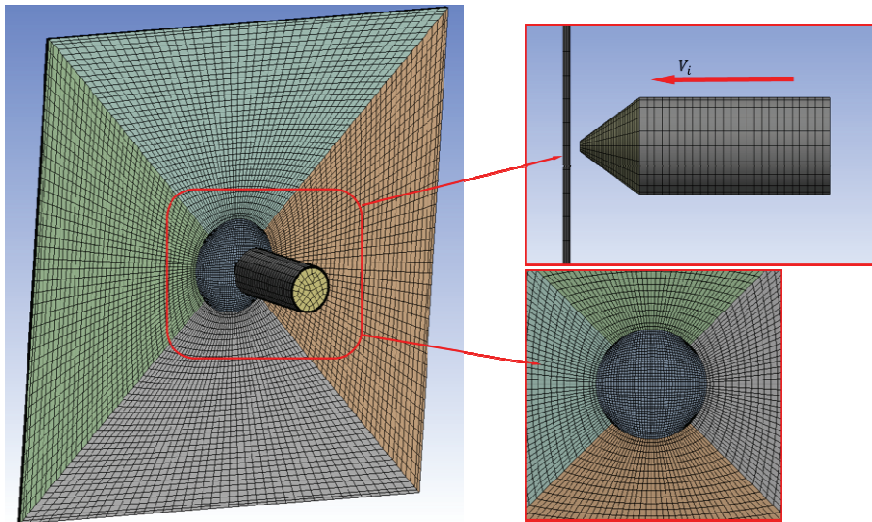
Fig. 12. 3D CAD model of steel plate and projectile used in numerical simulations

During computer calculations the steel sheets were fixed along the four sides of the specimen in order to model the boundary conditions used in the laboratory tests (full fixation).

The mesh size sensitivity took into consideration of the failure pattern and the value of the residual velocity. Thanks to this analysis, the optimal mesh is used in all simulations of the perforation problem. The following number of elements was used:

- for discretization of the specimen: fine mesh in the middle: 15126 nodes, 17592 elements type Solid 185(8) (5 elements along the thickness, average element dimensions 0.5×0.5×0.2 mm); remaining part: 10120 nodes, 8458 elements type Solid 185(8) (5 elements along the thickness, 1.0×1.0×0.2 mm; both parts of the specimen were tied in the analysis, the refined mesh part has a form of a circle of 5 cm in diameter in the region of contact between the two acting bodies,
- for discretization of the projectile: 25246 nodes, 26050 elements.

The model has been discretized with solid elements because they better reflect the nature of the structure's work. The hourglass control was activated.

The friction between the projectile and the plate is an important parameter as discussed in [25–28]. It was assumed as constant and equal to 0.1 as reported in [29] to reflect the friction observed between the bodies. The general contact was used together considering interior contact surfaces created during failure or erosion of the mesh related to the material. The applied failure criterion is "Plastic Strain Failure". The erosion of the elements starts when the maximum equivalent plastic strain of 0.7 defined as critical is reached resulting in single elements elimination from the global mesh.

The analysis was assumed as pure mechanical including adiabatic heat effects defined by Quiney-Taylor coefficient assumed as a constant value of 0.9. The material parameters used are specific heat C_p = 380 J/kgK and density ρ = 8587 kg/m^3. The initial temperature T_0 was varying during the calculations. The range of initial temperatures T_0 reflected the tests i.e. 293–573 K.

The simulations required a performant material model to correlate between the laboratory and numerical calculations. The Johnson-Cook [30] constitutive hardening relation was proposed to describe the dynamic material behavior of S235 steel. This elasto-thermo-viscoplastic material model described by the Eq. (1) determines the strain and strain rate hardening and thermal softening of the material. In Eq. (1), (A) is the yield stress, (B) and (n) are the strain hardening coefficients, (C) is the strain rate sensitivity coefficient, ($\dot{\varepsilon}_0$) is strain rate reference value and (m) is the temperature sensitivity parameter. The last bracket in Eq. (1), describes the thermal softening of the material and reduces the limit of the Mises equivalent stress ($\bar{\sigma}$) from the reference value at temperature (T_0) to zero at melting temperature (T_m).

$$(1) \qquad \bar{\sigma}\left(\bar{\varepsilon}_{pl}, \dot{\bar{\varepsilon}}_{pl}, T\right) = \left(A + B\bar{\varepsilon}_{pl}{}^n\right)\left(1 + C \ln\frac{\dot{\bar{\varepsilon}}_{pl}}{\dot{\varepsilon}_0}\right)\left[1 - \left(\frac{T - T_0}{T_m - T_0}\right)^m\right]$$

The Johnson-Cook constitutive constants were approximated using available data from static and dynamic tensile tests reported before, they are presented in Fig. 13 for the strain rate from 1 up to 3000 1/s. It is to be noted that the static tests were done using MTS tensile testing machine, whereas the dynamic tests were conducted using the Split Tensile Hopkinson Bar set-up.
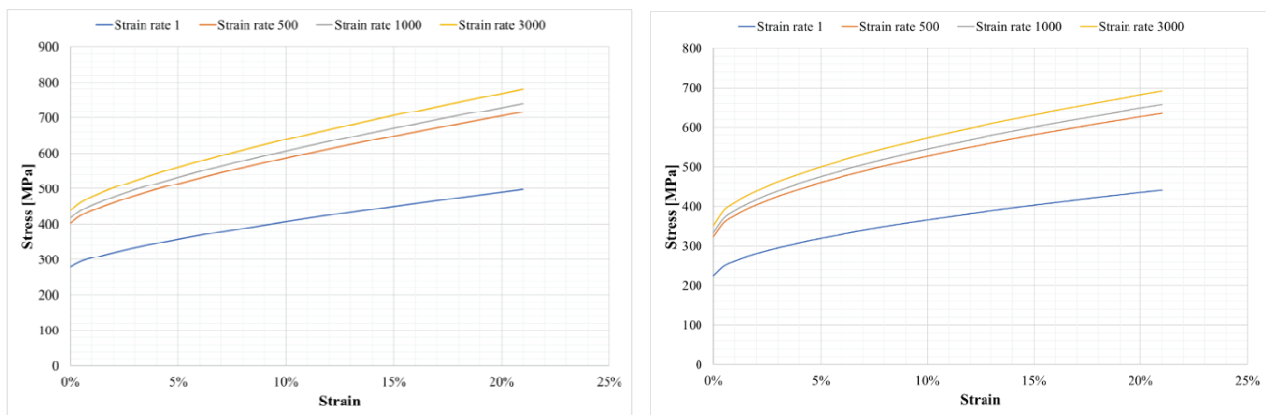
a)   b)

Fig. 13. True plastic stress-strain curve calculated according to Johnson Cook material model used during numerical simulations; a) initial temperature T_0 = 293 K (20°C), b) initial temperature T_0 = 573 K (300°C)

The constants of Johnson-Cook constitutive model adopted for calculation were: $A = 280$ MPa, $B = 667$ MPa, $n = 0.72$, $C = 0.071$, $m = 1.3$. As there were no own tests available for higher temperatures, the approximate material properties were adopted from [31]. The steel resistance capacity is reduced by 20% between $T = 293$ K and $T = 573$ K. In order to define the failure mode, the classical Johnson–Cook failure model [32, 33] was first studied. As demonstrated by closer analysis, the strain rate and temperature effect on the failure criterion is marginal within the studied range of strain rates and temperatures; therefore, a simplified version was adopted in the form of the constant equivalent plastic strain at failure. The parametrical analysis of the effective failure criterion consisted of observing the failure modes (petaling) and fitting the numerical ballistic curves to the experimental ones. As a result as previously stated, the value adopted for the equivalent plastic strain at failure is equal to 0.7.

4.2. Numerical results

The comparison of numerical calculations with laboratory tests data are presented in Fig. 14.
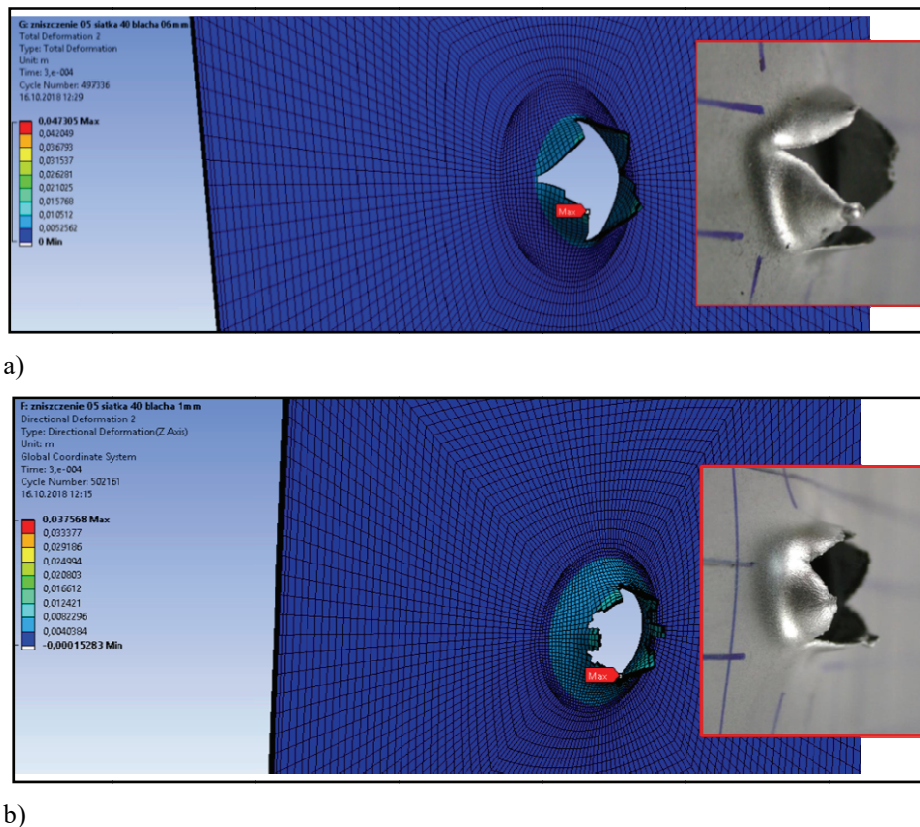

a)

b)

Fig. 14. View of the perforation areas – comparison between experimental and numerical findings; a) specimen thickness 0.6 mm, b) specimen thickness 1.0 mm

In both cases (numerical calculations, laboratory tests), the same characteristic 4 petals in the region of perforation are observed, this confirms the correctness of the constitutive law and failure criterion used. The results of the computer simulations were also used to analyze the kinetic energy dissipation during the perforation the steel sheet. These results were compared with laboratory tests data. The comparison study is presented in Fig. 15.

Results of laboratory experiments

Shot Pressure [bar]	Test No	T [K]	V0 [m/s]	t[ms]	VR[m/s]	%Energy change
2	T2	297	64.93	-	0	100%
3	T3	297	79.11	0.00	0	100%
3.2	T6	297	83.06	2.40	20.8	75%
4	T1	297	90.25	1.00	50	45%
5	T4	297	101.21	0.78	64.1	37%
7.5	T5	297	121.96	0.54	92.6	24%

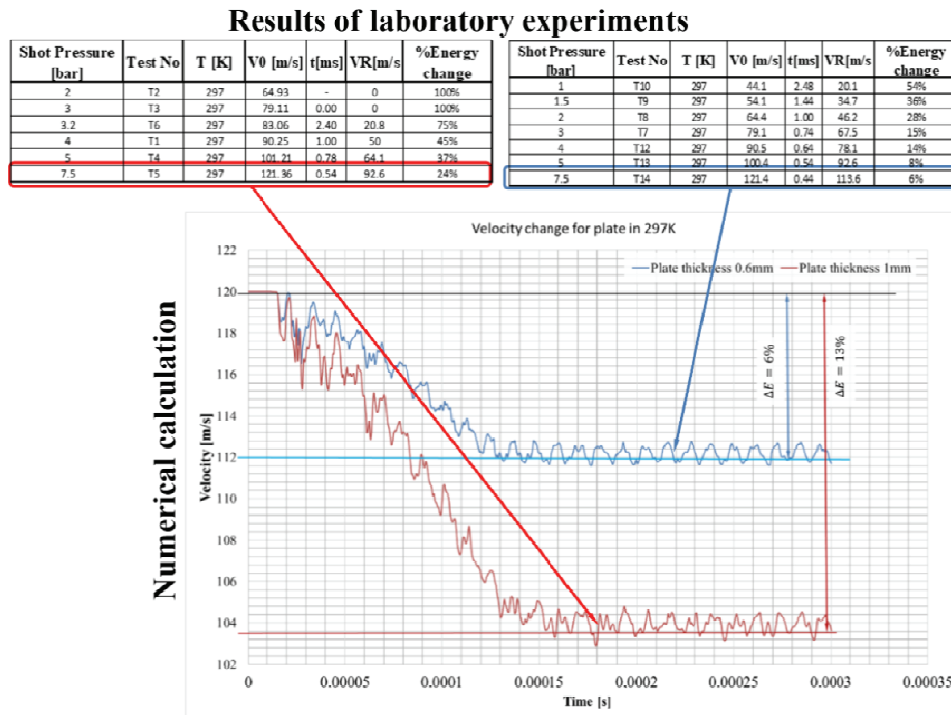| Shot Pressure [bar]	Test No	T [K]	V0 [m/s]	t[ms]	VR[m/s]	%Energy change
1	T10	297	44.1	2.48	20.1	54%
1.5	T9	297	54.1	1.44	34.7	36%
2	T8	297	64.4	1.00	46.2	28%
3	T7	297	79.1	0.74	67.5	15%
4	T12	297	90.5	0.64	78.1	14%
5	T13	297	100.4	0.54	92.6	8%
7.5	T14	297	121.4	0.44	113.6	6%

Fig. 15. Kinetic energy dissipation observed in numerical simulations and laboratory tests

A good correlation between results calculated by FEM method and obtained from laboratory experiments is observed, for the steel sheets of 1.0 mm thickness this accordance is slightly better. The kinetic energy dissipation calculated by FEM method is 13% and laboratory experiments show the dissipation of the order of 24%.

The numerical simulation results were also compared with the laboratory experiment results in terms of deformation shape, this is shown in Fig. 16.

The steel plate deformation value was compared for several path positions. The paths were located at the distance of 10, 20, 30, 40 and 50 mm from steel plate edge. Very small differences between numerical calculation and laboratory test results were observed, the maximum differences did not exceed 0.5 mm. These differences may be related to the failure criteria used during numerical simulation. Further improvements of the failure criterion could be considered.
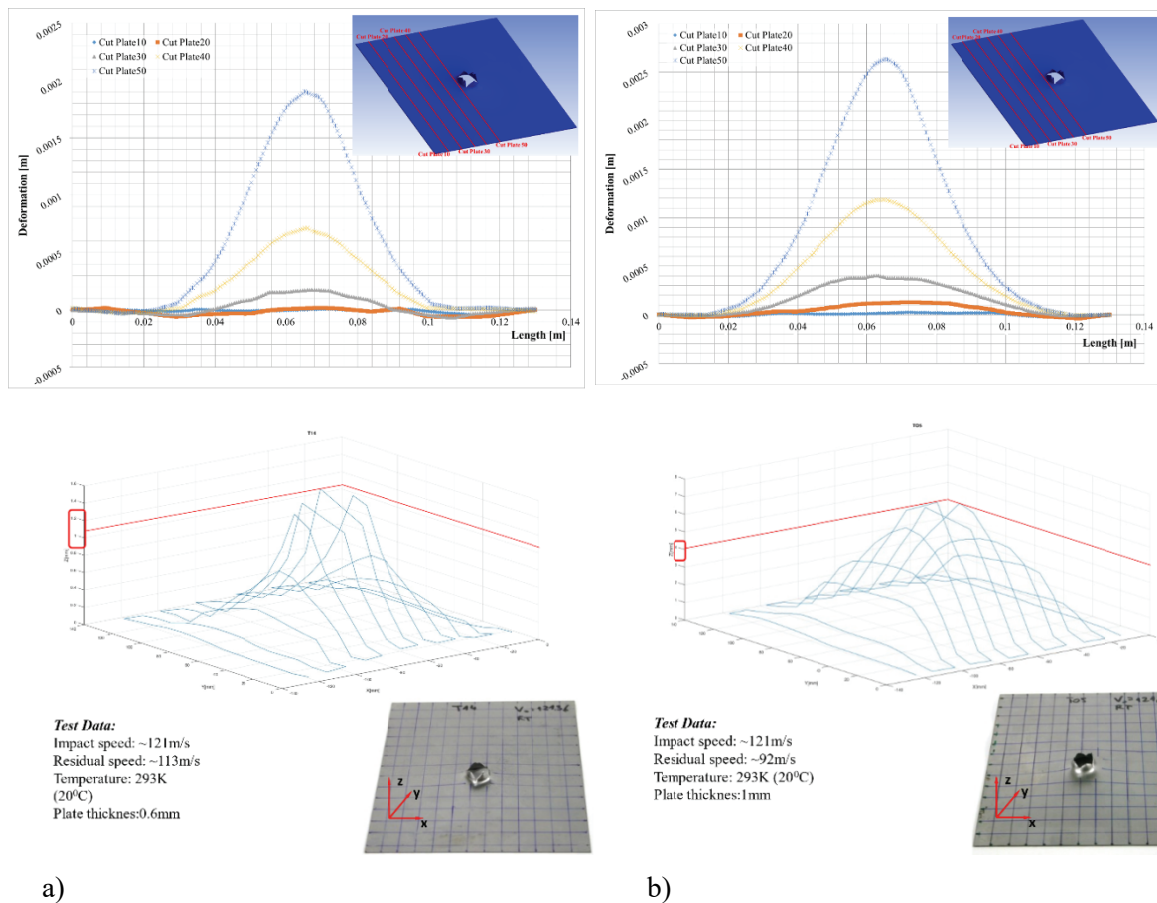
Fig. 16. Specimen deformation - numerical simulations vs. laboratory results; a) plate thickness of 0.6 mm, b) plate thickness of 1.0 mm

5. Conclusions

The paper presents results of laboratory tests and complementary numerical simulations by FEM method. The S235 steel specimens were tested using different experimental techniques to investigate the protective capacity of this metal against dynamic loading. The present results produce interesting conclusions for the design of building panels, protective partition walls of critical infrastructure facilities made of steel sheets and subjected to perforation in high temperature (e.g. fire) conditions. The material did not demonstrate any important anisotropy. The implemented Johnson-Cook constitutive relation in the FEM analysis combined with the proposed effective failure criterion allowed to reproduce experimental findings. The typical failure mode was observed with the same number of 3–4 petals as it was registered during the tests. It would be interesting to extend numerical simulations through an analysis of the perforation angle (other than 90°) of the impacting projectile in order to model more realistically the perforation of critical infrastructure

elements such as ricochet. The obtained results as well as the presented methodology of testing and numerical analysis are important elements to help the design of building panels and protective partitions of critical infrastructure facilities made of steel sheets. The laboratory perforation tests at elevated temperatures allowed for the scaling of the thermal component of the Johnson Cook model used in the numerical calculations. As numerical results correspond to the experimental findings, it can be concluded that the determined form of the thermal weakening coefficient allows to extrapolate the use of the proposed Johnson Cook model for higher temperatures and make it possible to determine perforation resistance in fire conditions and in case of blast.

Acknowledgments:

References

[1]   M. Grazka, L. Kruszka, W. Mocko and M. Klosak, "Advanced Experimental and Numerical Analysis of Behavior Structural Materials Including Dynamic Conditions of Fracture for Needs of Designing Protective Structures", in Soft Target Protection, NATO Science for Peace and Security Series C: Environmental Security, Springer, 2020, pp. 121–137. https://doi.org/10.1007/978-94-024-1755-5_10

[2]   N. Jones, and J. Paik, "Impact perforation of aluminium alloy plates", *International Journal of Impact Engineering*, vol. 48, pp. 46–53, 2012. https://doi.org/10.1590/S1679-78252013000400006

[3]   L. Kruszka and R. Rekucki, "Experimental Analysis of Impact and Blast Resistance for Various Built Security Components", in Soft Target Protection. NATO Science for Peace and Security Series C: Environmental Security, L. Hofreiter, V. Berezutskyi, L. Figuli, Z. Zvaková (eds). Springer, Dordrecht, pp. 211–239, 2020. https://doi.org/10.1007/978-94-024-1755-5_18

[4]   Council Directive 2008/114/EC of 8 December 2008 on the identification and designation of European critical infrastructures and the assessment of the need to improve their protection, European Union, 2008.

[5]   L. Kruszka and Z. Kubíková, "Critical Infrastructure Systems Including Innovative Methods of Protection", in *Critical Infrastructure Protection. NATO Science for Peace and Security Series D: Information and Communication Security*, L. Kruszka, M. Klosak, P. Muzolf P. (eds), IOS Press, Amsterdam, 2019.

[6]   L. Kruszka and R. Rekucki, "Performance of protective doors and windows under impact and explosive loads", Applied Mechanics and Materials, vol. 82, pp. 422–427, 2011. https://doi.org/10.4028/www.scientific.net/AMM.82.422

[7]   European Standard EN10025:2004.

[8]   M. Klosak, A. Rusinek, A. Bendarma, T. Jankowiak and T. Lodygowski, "Experimental study of brass properties through perforation test using a thermal chamber for elevated temperatures", *Latin American Journal of Solid and Structures*, vol. 15, no 10, 2018. https://doi.org/10.1590/1679-78254346

[9]   T. Jankowiak, A. Rusinek, K.M. Kpenyigba and R. Pesci, "Ballistic behaviour of steel sheet subjected to impact and perforation", Steel and Composite Structures, vol. 16, no 6, pp. 595–609, 2014. https://doi.org/10.12989/scs.2014.16.6.595

[10]   A. Rusinek, J.A. Rodrıguez-Martınez, R. Zaera, J.R. Klepaczko, A. Arias and C. Sauvelet, "Experimental and numerical study on the perforation process of mild steel sheets subjected to perpendicular impact by hemispherical projectiles", *International Journal of Impact Engineering*, vol. 36, no 4, pp. 565–587, 2009. https://doi.org/10.1016/j.ijimpeng.2008.09.004

[11]   W. Mocko, J. Janiszewski, J. Radziejewska and M. Grazka, „Analysis of deformation history and damage initiation for 6082-T6 aluminium alloy loaded at classic and symmetric Taylor impact test conditions", *International Journal of Impact Engineering*, vol. 75, pp. 203–213, 2015. https://doi.org/10.1016/j.ijimpeng.2014.08.015

[12]   M. Grazka and J. Janiszewski, "Identification of Johnson-Cook equation constants using finite element method", *Engineering Transactions*, vol. 60, no 3, pp. 215–223, 2012.

[13]   R. Panowicz, J. Janiszewski and K. Kochanowski, "The influence of non-axisymmetric pulse shaper position on SHPB experimental data", *Journal of Theoretical and Applied Mechanics*, vol. 56, no 3, pp. 873–886, 2017. https://doi.org/10.15632/jtam-pl.56.3.873

[14]   L. Kruszka and J. Janiszewski, "Experimental analysis and constitutive modelling of steel of A-IIIN strength class", *EPJ Web of Conferences*, vol. 94, 05007, 2015. https://doi.org/10.1051/epjconf/20159405007

[15]   A. Rusinek, R. Bernier, R. Matadi Boumbimba, M. Klosak, T. Jankowiak and G.Z. Voyiadjis, "New device to capture the temperature effect under dynamic compression and impact perforation of polymers, application to PMMA", *Polymer testing*, vol. 65, pp. 1–9, 2018. https://doi.org/10.1016/j.polymertesting.2017.10.015

[16]   A. Bendarma, T. Jankowiak, T. Łodygowski, A. Rusinek and M. Klosak, "Experimental and numerical analysis of the aluminum alloy AW5005 behaviour subjected to tension and perforation under dynamic loading", Journal of Theoretical and Applied Mechanics, vol. 55, no 4, pp. 1219–1233, 2016. https://doi.org/10.15632/jtam-pl.55.4.1219

[17]   T. Børvik, O,S. Hopperstad, M. Langseth and K.A. Malo, "Effect of target thickness in blunt projectile penetration of Weldox 460 E steel plates", *International Journal of Impact Engineering*, vol. 28, no 4, pp. 413–464, 2003. https://doi.org/10.1016/S0734-743X(02)00072-6

[18]   T. Jankowiak, A. Rusinek and P. Wood, "A numerical analysis of the dynamic behaviour of sheet steel perforated by a conical projectile under ballistic conditions", *Finite Elements in Analysis and Design*, vol. 65, pp. 39-49, 2013. https://doi.org/10.1016/j.finel.2012.10.007

[19]   B. Landkof and W. Goldsmith, "Petaling of thin metallic plates during penetration by cylindro-conical projectiles", *International Journal of Solids and Structures*, vol. 21, no 3, pp. 245–266, 1985. https://doi.org/10.1016/0020-7683(85)90021-6

[20]   K.M. Kpenyigba, T. Jankowiak, A. Rusinek and R. Pesci, "Influence of projectile shape on dynamic behaviour of steel sheet subjected to impact and perforation", *Thin-Walled Structures*, vol. 65, pp. 93-104, 2013. https://doi.org/10.1016/j.tws.2013.01.003

[21]   Z. Wei, D. Yunfei, C. Zong Sheng and W. Gang, "Experimental investigation on the ballistic performance of monolithic and layered metal plates subjected to impact by blunt rigid projectiles", International Journal of Impact Engineering, vol. 49, pp. 115–129, 2012. https://doi.org/10.1016/j.ijimpeng.2012.06.001

[22]   R.F. Recht and T.W.Ipson, "Ballistic perforation dynamics", *Journal of Applied Mechanics*, vol. 30, no 3, pp. 384–390, 1963. https://doi.org/10.1115/1.3636566

[23]   J.K. Holmen, O.S. Hopperstad and T. Børvik, "Influence of yield-surface shape in simulation of ballistic impact", *International Journal of Impact Engineering*, vol. 108, pp. 136–146, 2017. https://doi.org/10.1016/j.ijimpeng.2017.03.023

[24]   A. Arias, J.A. Rodríguez-Martínez and A. Rusinek, "Numerical simulations of impact behaviour of thin steel plates subjected to cylindrical, conical and hemispherical non-deformable projectiles", *Engineering Fracture Mechanics*, vol. 75, pp. 1635–1656, 2008. https://doi.org/10.1016/j.engfracmech.2007.06.005

[25]   A. Massaq, A. Rusinek, M. Klosak, F. Abed and M. El Mansori, "A study of friction between composite-steel surfaces at high impact velocities", *Tribology International*, vol. 102, pp. 38–43, 2016. https://doi.org/10.1016/j.triboint.2016.05.011

[26]   M. Klosak, T. Jankowiak, A. Rusinek, A. Bendarma, P.W. Sielicki and T. Lodygowski, "Mechanical Properties of Brass under Impact and Perforation Tests for a Wide Range of Temperatures: Experimental and Numerical Approach", *Materials*, vol. 13, no 24, 5821, 2020. https://doi.org/10.3390/ma13245821

[27]   S.C. Lim, M.F. Ashby and J.H. Brunton, "The effects of sliding conditions on the dry friction of metals", *Acta Metallurgica*, vol. 37, no 3, pp. 767-772, 1989. https://doi.org/10.1016/0001-6160(89)90003-5

[28]   Z. Rosenberg and Y. Vayig, "On the friction effect in the perforation of metallic plates by rigid projectiles", *International Journal of Impact Engineering*, vol. 149, 103794, 2021. https://doi.org/10.1016/j.ijimpeng.2020.103794

[29]   Friction and Friction Coefficients, www.engineeringtoolbox.com [access 2018-03-03].

[30]   G.R. Johnson and W.H. Cook, "A constitutive model and data for metals subjected to large strains, high strain rates and high temperatures", in *Proceedings of the 7th International Symposium on Ballistics*, vol. 21, pp. 541–547, 1983.

[31]   W. Ciolek, „Stal budowlana w temperaturach pożarowych w świetle Eurokodów – cz II (in Polish)", *Inżynier Budownictwa*, vol. 4, pp. 89–93, 2015.

[32]   G.R. Johnson and W.H. Cook, "Fracture characteristics of three metals subjected to various strains, strain rates, temperatures and pressures", *Engineering Fracture Mechanics*, vol. 21, pp. 31–48, 1985. https://doi.org/10.1016/0013-7944(85)90052-9

[33]   G.R. Johnson and T.J. Holmquist, "Test Data and Computational Strength and Fracture Model Constants for 23 Materials Subjected to Large Strains, High Strain Rates, and High Temperatures", Los Alamos National Laboratory, Los Alamos, NM, USA. 1989.

Analiza perforacji arkuszy stali S235 w temperaturach do 573 K metodą eksperymentalną i numeryczną

Streszczenie:

W artykule opisano efektywne techniki eksperymentalne i numeryczne stosowane w projektowaniu konstrukcjo ochronnych budowlanej infrastruktury krytycznej. Bezpieczeństwo infrastruktury krytycznej stało się poważniejszym problemem w czasach rosnących zagrożeń terrorystycznych. Infrastruktura krytyczna odnosi się do obiektów budowlanych i ich elementów, w tym w szczególności do budowli związanych z wytwarzaniem, przesyłem i dystrybucją energii elektrycznej, paliw, ropy naftowej i produktów ropopochodnych, sieci telekomunikacyjnych i wodociągowych, zakładów produkcji i dystrybucji żywności, elektrociepłowni, obiektów ochrony zdrowia (szpitale), komunikacyjnych (drogi, koleje, lotniska, porty morskie), instytucji finansowych i służby bezpieczeństwa (policja, wojsko, ratownictwo). Tak więc infrastruktura krytyczna to nie tylko budynki wojskowe, ale także obiekty użyteczności publicznej, które wykonane są z typowych materiałów budowlanych, takich jak użyta w prezentowanych badaniach stal S235. Ich konstrukcje zabezpieczające powinny spełniać warunek niezawodności jak dla konstrukcji inżynierskich, dla których zostały w pełni określone właściwości ochronne materiałów konstrukcyjnych. Należy zauważyć, że zagrożenie dla krytycznych elementów infrastruktury zwykle nie pochodzi z bezpośredniego ataku rakietowego, ale jest spowodowane głównie przez odłamki z eksplozji lub w wyniku rykoszetu. Ponieważ cały budynek nie może być chroniony przed atakiem rakietowym, inżynierowie projektują specjalne wzmocnienia składające się z metalowych paneli lub elementów kompozytowych na drzwi, ściany itp. Tutaj zastosowanie znajdują blachy stalowe S235, których właściwości użytkowe są korzystne dla rozwoju zastosowań inżynierskich w dziedzinie ochrony infrastruktury krytycznej.

Badany materiał, czyli stal S235, jest typowym materiałem konstrukcyjnym, zaś przedstawione wyniki uzyskano z eksperymentów perforacji wykonanych na blachach S235 poddanych uderzeniom charakteryzującym się umiarkowaną prędkością (około 40–120 m/s). Kwadratowe próbki o wymiarach 13×13 cm i grubościach 0,6 mm i 1,0 mm, mocowane sztywno wzdłuż czterech krawędzi, poddawane są procesowi perforacji z użyciem pocisku o zakończeniu stożkowym i masie 28 g, wykonanego ze słabo odkształcalnej stali maraging. Oryginalność badań perforacji polega na zastosowaniu komory termicznej przeznaczonej do przeprowadzania eksperymentów w wyższych temperaturach. Komora termiczna pozwala na równomierne ogrzanie próbki do wymaganej temperatury, w przypadku prezentowanej analizy do 573 K (300°C), po którym następuje uwolnienie pocisku. W celu określenia energii rozproszonej podczas perforacji dokonywane są pomiary prędkości początkowej V_0 (uderzenia badanej próbki) oraz rezydualnej V_R (po perforacji) za pomocą urządzeń laserowych. Próbki poddawane są analizie pod kątem modelu zniszczenia – dla metali i pocisków o zakończeniu stożkowych najczęstszą formą są tzw. petals. Do ostatecznych pomiarów deformacji kształtu wykorzystano skanery 3D i sterowane numerycznie urządzenia pomiarowe (technologia pomiarów CNC). Stal została przetestowana również przy użyciu techniki pręta Hopkinsona i uzyskane wyniki pozwoliły na określenie dynamicznych właściwości mechanicznych tego materiału. Ważnym elementem badań jest analiza numeryczna metodą elementów skończonych. Wykorzystano program Ansys i jego solver oparty o algorytmy jawnego całkowania równań. Model zbudowano z trójwymiarowych elementów typu Solid. Zaproponowany model konstytutywny Johnsona Cooka oparto na dostępnych danych materiałowych, wprowadzając zależność materiału od temperatury i szybkości odkształcenia. Zastosowane jednowymiarowe kryterium zniszczenia polega na usuwaniu z modelu elementów, które osiągają zadaną krytyczną wartość odkształceń plastycznych, wynoszącą 0,7.

Uzyskane wyniki eksperymentalne pozwoliły określić użytkowe właściwości balistyczne materiału, czyli zależność prędkości początkowej V_0 i rezydualnej V_R oraz limit balistyczny. Limit balistyczny obniża się ze wzrostem temperatury. Model MES odzwierciedlił z powodzeniem zachowanie próbek podczas eksperymentu zarówno w zakresie formy zniszczenia, jak i parametrów balistycznych.